J Therm Anal Calorim (2009) 97:215–221
DOI 10.1007/s10973-009-0263-5

Heating rate effect on the thermal behavior of ammonium nitrate and its blends with limestone and dolomite

T. Kaljuvee · I. Rudjak · E. Edro · A. Trikkel

ICTAC2008 Conference

Abstract The effect of heating rate on the thermal behavior of ammonium nitrate (AN) and on the kinetic parameters of decomposition of AN and its blends with limestone and dolomite was studied on the basis of commercial fertilizer-grade AN and several Estonian limestone and dolomite samples. Experiments were carried out under dynamic heating conditions up to 900 °C at heating rates of 2, 5, 10 and 20 °C min^{-1} in a stream of dry air using Setaram Labsys 2000 equipment. For calculation of kinetic parameters, the TG data were processed by differential isoconversional method of Friedman. The variation of the value of activation energy E along the reaction progress α showed a complex character of decomposition of AN—interaction of AN with limestone and dolomite additives with the formation of nitrates as well as decomposition of these nitrates at higher temperatures.

Keywords Ammonium nitrate · Dolomite · Kinetics · Limestone · TG–DTA · Thermal stability

Introduction

The kinetics of decomposition (gasification) of AN in solid [1–5] and liquid phase [1, 6–8] as well as of phase stabilized AN (PSAN) [9, 10] has been studied by several authors, but there is no data about AN blends with dolomite and limestone as additives.

Earlier, the influence of different lime-containing materials on the thermal behavior of ammonium nitrate (AN) was studied using combined TG–DTA–EGA (FTIR) equipment varying the amount of additives in a wide range from 5 mass% to mole ratio of AN/(CaO + MgO) = 2:1 [11].

The aim of this research was to study the effect of heating rate (non-isothermal conditions) on the thermal behavior of AN and on the kinetic parameters of decomposition of AN and its blends with limestone and dolomite.

Experimental

Materials

Commercial fertilizer-grade AN (34.4% N) (Tserepovetski Azot Ltd, Russia) was under investigation. Three Estonian limestone (from Võhmuta, Vasalemma, and Karinu deposits) and three dolomite (Kurevere, Anelema and Anelema wastes) previously ground (<45 μm) samples were used as additives to AN. Anelema wastes were obtained as a fine fraction from rubble manufacturing. The chemical composition and specific surface area (SSA) of the limestone and dolomite samples are presented in Table 1. The content of total CaO in limestone was 52.9–54.2 mass% and of total MgO 1.1–2.8 mass%. In dolomite samples, the content of total CaO was in between 26.0 and 29.0 mass% and of total MgO 24.3–26.6 mass%. The content of insoluble residue in limestone samples was 0.8–1.3 mass%, in Kurevere and Anelema dolomite samples 3.2 and 5.8 mass%, respectively, and in Anelema wastes 12.4 mass%. The SSA of the samples studied was relatively small (from 0.74 to 2.44 $m^2\ g^{-1}$), being somewhat bigger for dolomite samples.

More precise characterization of limestone and dolomite samples used has been presented in [11] showing that all

T. Kaljuvee (✉) · I. Rudjak · E. Edro · A. Trikkel
Laboratory of Inorganic Materials, Tallinn University of Technology, Ehitajate tee 5, 19086 Tallinn, Estonia
e-mail: tiidu@staff.ttu.ee

Table 1 Chemical composition and specific surface area (SSA) of limestone and dolomite samples

Sample	Chemical composition (mass %)[a]							BET SSA (m^2 g^{-1})
	CaO	MgO	CO_2	I.R.[b]	Al_2O_3	Fe_2O_3	$S_{sulphate}$	
Karinu	52.92	2.76	38.98	0.80	1.72	0.08	0.04	0.74
Võhmuta	53.17	1.50	39.87	1.33	1.81	0.04	0.06	1.56
Vasalemma	54.22	1.14	40.45	0.75	1.50	0.09	0.09	0.89
Kurevere	29.04	24.40	41.87	3.17	0.64	0.21	0.09	1.70
Anelema	28.85	26.63	40.81	5.83	0.84	0.14	0.10	2.44
Anelema wastes	25.95	24.29	35.58	12.41	1.41	0.37	0.10	5.79

[a] Per dry mass

[b] Insoluble residue in aqua regia

samples except Anelema wastes were relatively pure limestone and dolomite.

Methods

To study the effect of heating rate on thermal stability of AN, thermogravimetric equipment (Setaram Labsys 2000) capable of simultaneous recording of mass loss (TG), differential mass loss (DTG) and differential thermal analyses curve (DTA) was used. The experiments were carried out under dynamic heating conditions from 30 to 900 °C, or in the case of neat AN to 400 °C, at heating rates of 2, 5, 10 and 20 °C min^{-1} in a stream of dry air (flow rate 120 mL min^{-1}). Standard 100 µL alumina crucibles were used. Sample mass was calculated on the basis of constant mass of AN (6 ± 0.2 mg), the content of additives in the blends was 20 mass%.

Results and discussion

Thermal analysis

No systematic dependence of the temperatures of endoeffect minimums on DTA curves corresponding to the principal transitions of $AN_{IV} \leftrightarrow AN_{III} \leftrightarrow AN_{II} \leftrightarrow AN_{I}$ on the heating rate were fixed. The most evident phenomenon was that at lower heating rates these endoeffects occurred at higher temperatures, but the transition of $AN_{I} \leftrightarrow AN_{melt}$ was always shifted towards higher temperatures at higher heating rates.

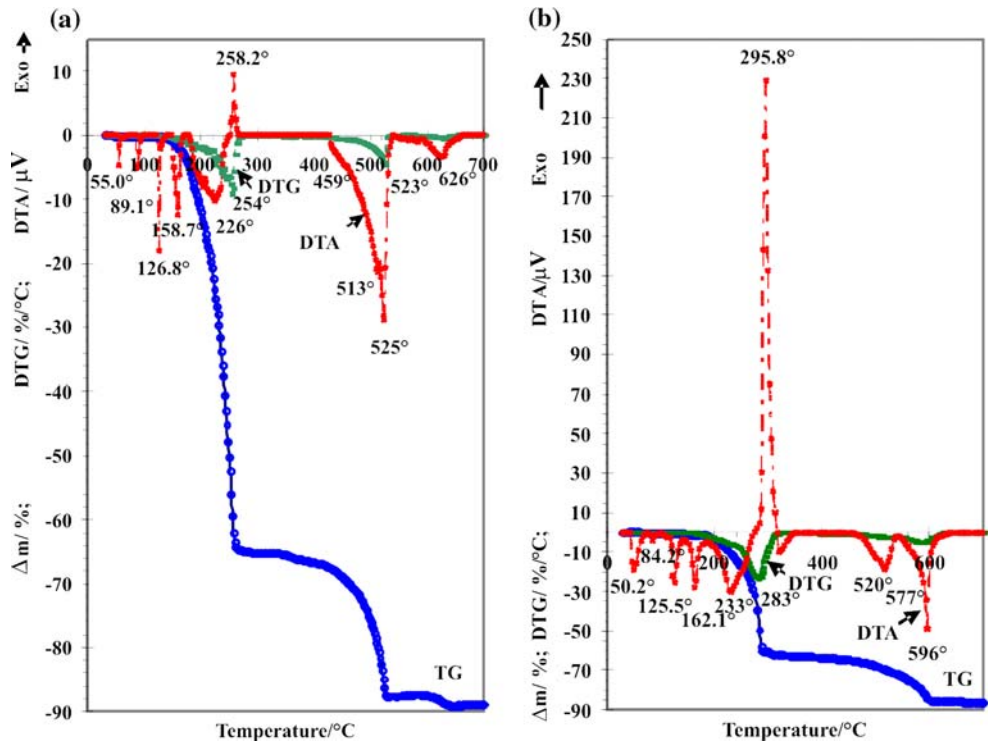

Fig. 1 Thermal analysis curves of AN blend with Vasalemma limestone at a heating rate of 2 °C min^{-1} (**a**) and 20 °C min^{-1} (**b**)

For example, for neat AN at the heating rates of 2 and 20 °C min^{-1} the peaks of phase transitions of $AN_{IV} \leftrightarrow AN_{III} \leftrightarrow AN_{II} \leftrightarrow AN_{I}$ on the DTA curves were fixed, respectively, at 53.7 and 52.2 °C, 90.4 and 86.4 °C, 126.1 and 127.1 °C, but of $AN_{I} \leftrightarrow AN_{melt}$ at 165.2 and 167.2 °C. For the blend of AN with 20% Vasalemma limestone these transitions at the heating rates of 2 °C min^{-1} (Fig. 1a) and 20 °C min^{-1} (Fig. 1b) occurred at 55.0 and 50.2 °C, 89.1 and 84.2 °C, 126.8 and 125.5 °C, respectively, and of $AN_{I} \leftrightarrow AN_{melt}$ at 158.7 and 162.1 °C.

At higher temperatures and in the case of neat AN these phase transitions were followed at the heating rates of 2, 5, 10 and 20 °C min^{-1} by the decomposition exotherm of AN with maximums on the DTA curve respectively at 239.6, 258.8, 262.9 °C (shoulders at 229 and 245 °C) and 282.9 °C (shoulder at 258 °C), thereby, the higher the heating rate the more intensive the exotherm was (Fig. 2a).

At thermal treatment of AN blends with limestone or dolomite additives a multi-peaked endotherm was fixed on the DTA curves in the temperature interval of 180–280 °C, characterizing interaction of AN with $CaCO_3$ and $MgCO_3$*$CaCO_3$ from natural limestone and dolomite leading to the formation of calcium and magnesium nitrates [11]. This endoeffect was followed, as a rule, by a more or less intensive exoeffect, characterizing the decomposition of residual AN. The decomposition exotherm of AN was shifted towards higher temperatures and the intensities of exotherms at that were much smaller as compared to neat AN. At the heating rate of 2 °C min^{-1}, it was especially miserable or missing at all.

For example, at the heating rate of 2 °C min^{-1} for AN with Vasalemma limestone additive an endotherm with minimum at 226 °C was fixed on the DTA curve, which was followed by a weak exoeffect with maximum at 258.2 °C (Fig. 1a). The total mass loss at heating up to 315 °C was 65.1%. At the heating rate of 20 °C min^{-1} the endo- and exoeffect (the last one very intensive), were fixed with minimum at 233 °C and maximum at 295.8 °C, respectively, and the total mass loss at heating up to 320 °C was 62.0% (Fig. 1b). For the AN blend with Võhmuta limestone, the decomposition exotherm of AN at the heating rate of 2 °C min^{-1} was missing and the maximum of the exotherm on the DTA curve at heating rates of 5, 10 and 20 °C min^{-1} was shifted, respectively, 4.0, 11.4 and 30.9 °C towards higher temperatures as compared to neat AN (Fig. 2a, b).

With the following increase in temperature the endotherms in between 350 and 600 °C characterized the decomposition of previously formed $Mg(NO_3)_2$ and $Ca(NO_3)_2$ and in between 600 and 700 °C the decomposition of residual carbonates. On the DTA curve of AN with Vasalemma limestone additive at the heating rate of 2 °C min^{-1}, an endotherm with minimums at 513 and 525 °C, and with a shoulder at 459 °C, and another with minimum at 626 °C were fixed (Fig. 1a). The total mass loss at heating up to 535 and 700 °C was 87.5 and 89.0%, respectively. At the heating rate of 20 °C min^{-1} two endoeffects with minimums at 520 and 596 °C (and a shoulder at 577 °C) and no endotherms at higher temperatures were fixed on the DTA curve. The total mass loss at

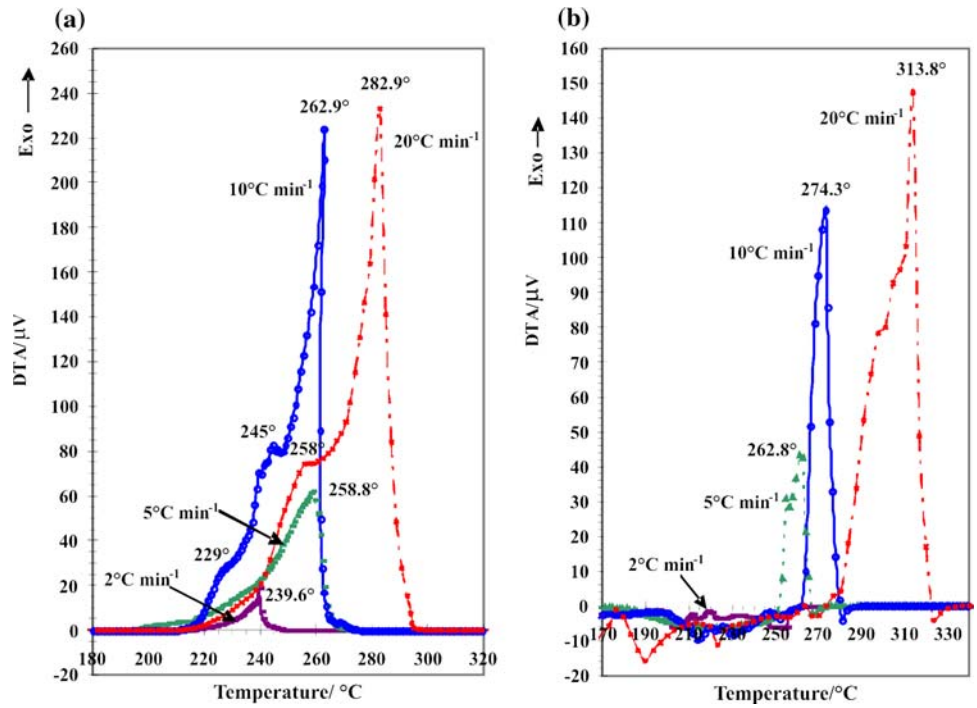

Fig. 2 DTA curves of neat AN (**a**) and AN blends with Võhmuta limestone (**b**) at different heating rates

heating up to 610 and 700 °C was 85.4 and 86.2% (Fig. 1b), respectively, which means that there was only a small amount of unreacted carbonates left.

Determination of kinetic parameters

The decomposition of AN and the interaction of AN with limestone or dolomite additives with formation of nitrates as well as the following decomposition of the nitrates at higher temperatures have a complicated multi-step mechanism (Figs. 1, 2). In such situation, the reaction rate can be described only by complex equations, where the activation energy E is no more constant but is dependent on the reaction progress α ($E = E(\alpha)$). The kinetic parameters are evaluated by isoconversional method which involves determination of temperatures corresponding to certain, arbitrarily chosen values of α recorded in the experiments carried out at different heating rates β [12–15].

The differential isoconversional method of Friedman [12] was used to calculate kinetic parameters from non-isothermal experiments. After baseline correction and normalization, the TG data obtained at different heating rates were processed with the AKTS Advanced Thermokinetics software [16].

From the generally accepted equation of the non-isothermal kinetics:

$$\beta\frac{\mathrm{d}\alpha}{\mathrm{d}T} = f(\alpha)A(\alpha)\exp\left(-\frac{E(\alpha)}{RT}\right) \quad (1)$$

where α is the degree of conversion, $f(\alpha)$ is the function dependent on the reaction mechanism, β is the heating rate, T is the temperature in K, A pre-exponent factor in s^{-1} and R is the gas constant, an equation corresponding to the Friedman's differential isoconversional method can be obtained as follows:

$$\ln\left(\beta\frac{d\alpha}{dT}\right) = \ln[A(\alpha)f(\alpha)] - \frac{E(\alpha)}{RT}. \quad (2)$$

Replacing $\beta(\mathrm{d}\alpha/\mathrm{d}T)$ with $\mathrm{d}\alpha/\mathrm{d}t$ in the Eq. 2, the Friedman analysis, based on the Arrhenius equation, applies the logarithm of the conversion rate $\mathrm{d}\alpha/\mathrm{d}t$ as a function of the reciprocal temperature at different degrees of conversion:

$$\ln\frac{\mathrm{d}\alpha}{\mathrm{d}t}\bigg|_{\alpha_i} = \ln[A_i f(\alpha_{i,j})] - \frac{E_i}{RT_{ij}}. \quad (3)$$

As the function dependent on the reaction model $f(\alpha)$ is assumed to be a constant at each conversion degree $\alpha_{i,j}$ (i—index of conversion; j—index of heating rate), the dependence of the logarithm of the reaction rate over $1/T$ is linear with the slope of E_i/R.

The reaction rates for the decomposition of neat AN and its blend with Vasalemma limestone with formation of nitrates at lower temperatures (step I) are presented in Fig. 3. The conversion rates ($\mathrm{d}\alpha/\mathrm{d}t$), measured at different temperatures for different heating rates allowed to determine the kinetic parameters A and E presented in Fig. 4 for the overall process as a function of reaction progress. The data for step II, decomposition of the nitrates formed at lower temperatures during step I, are presented in Fig. 5.

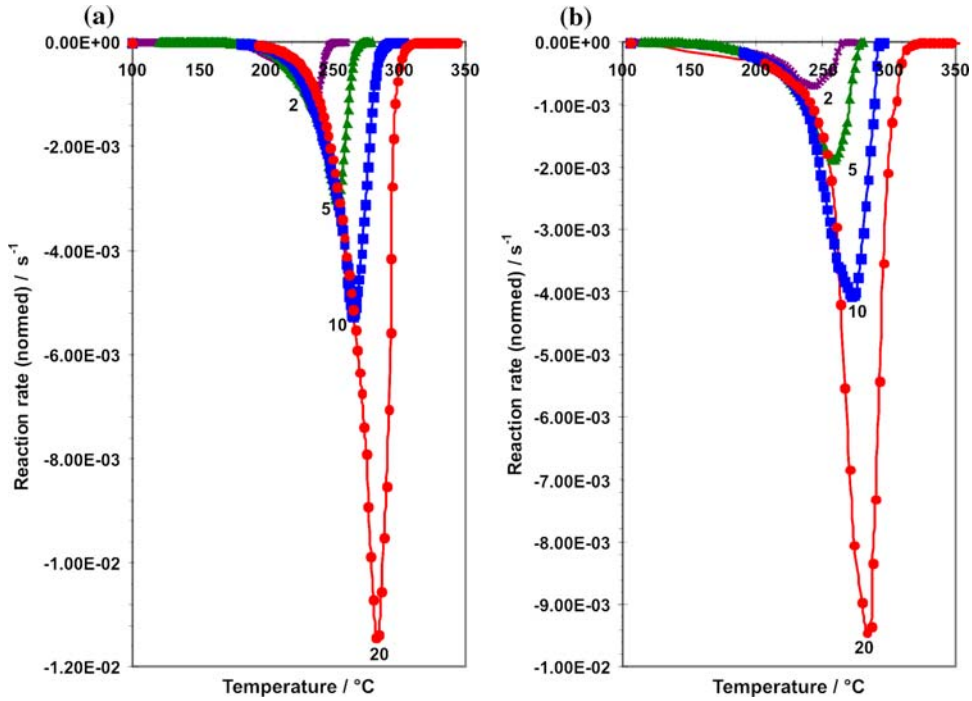

Fig. 3 Reaction rate $\mathrm{d}\alpha/\mathrm{d}t$ (DTG, normalized signals) for the decomposition of neat AN (**a**) and for the step I of AN blend with Vasalemma limestone (**b**) as a function of temperature for different heating rates. (The values of the heating rate in (°C min^{-1}) are marked on the curves)

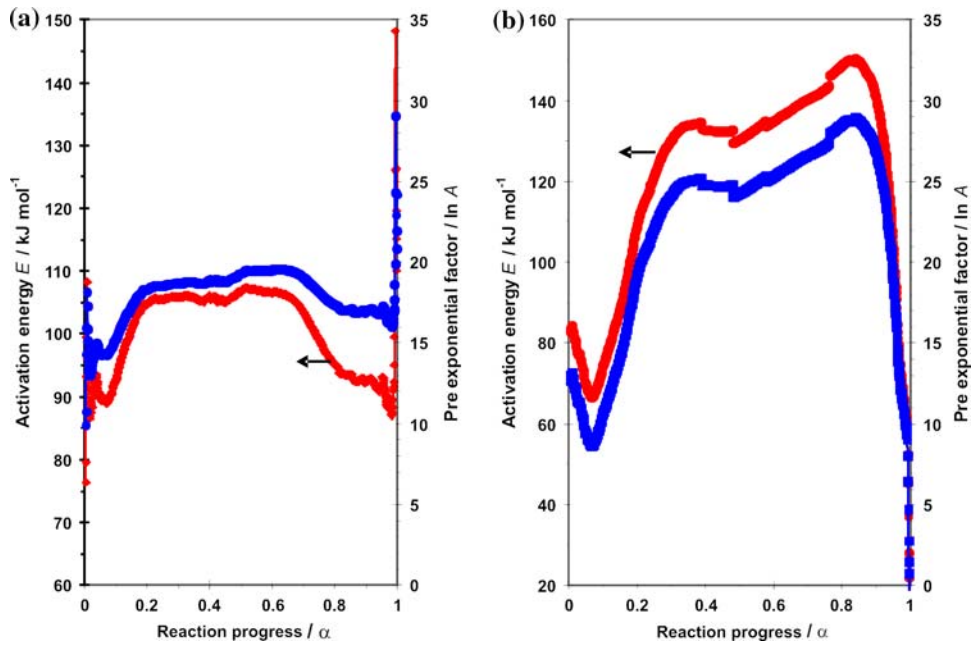

Fig. 4 Activation energy E and pre-exponential factor A determined by Friedman analysis as a function of the reaction progress for the decomposition of neat AN (**a**) and for the step I of AN blend with Vasalemma limestone (**b**)

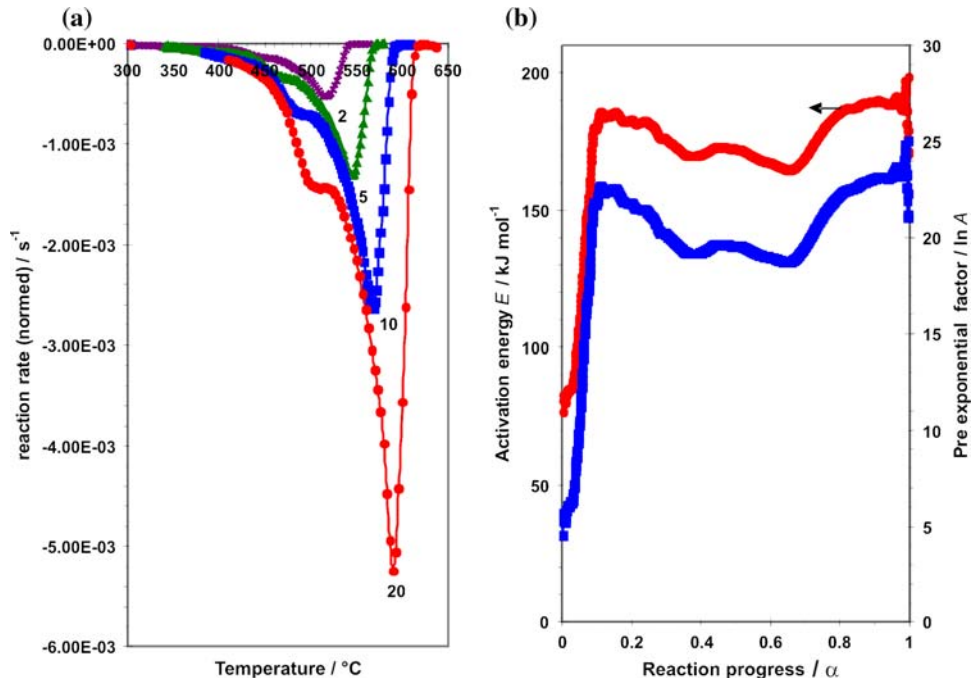

Fig. 5 Reaction rate dα/dt (**a**), activation energy E and pre-exponential factor A (**b**) for the step II of AN blend with Vasalemma limestone

The values of the activation energy for all the blends studied are presented in Table 2.

The results presented in Table 2, and in Fig. 4 and 5b express the complex character of the decomposition of AN and its interactions with limestone or dolomite additives as well as prove the formation (step I) and decomposition of nitrates (step II), whereas the values of activation energy and pre-exponential factor are visibly dependent on the reaction extent.

For neat AN, the activation energy in the range of conversion (decomposition) degree of $0.1 < \alpha < 0.9$ varies in between 92.4 and 106.8 kJ mole^{-1} (pre-exponential factor A from 4.41*10^6 to 2.94*10^8 s^{-1}) (Fig. 4a) being at that 0.9–12.9 kJ mole^{-1} higher than this calculated in [1] by DSC signals ($E = 92.7 \pm 1.2$ kJ mole^{-1}, sample mass $\sim$1 mg) using isoconversional method for non-isothermal gasification of AN.

For AN blends with limestone and dolomite the value of activation energy in the same range of α (decomposition and interactions of AN with limestone and dolomite additives—step I) varied much more than for neat AN. For example, for AN blend with Võhmuta limestone

Table 2 The activation energy E (kJ mole^{-1}) and pre-exponent factor ln A versus reaction progress α

Sample	α																	
	0.1		0.2		0.3		0.4		0.5		0.6		0.7		0.8		0.9	
	E	ln$A$	E	ln$A$	E	ln$A$	E	ln$A$	E	ln$A$	E	ln$A$	E	ln$A$	E	ln$A$	E	ln$A$
Step I																		
Neat AN	92.7	15.3	104.8	18.3	106.0	18.7	106.0	18.9	106.8	19.3	106.6	19.5	103.5	19.1	95.1	17.4	92.4	17.0
AN + 20% Võhmuta	58.5	7.2	76.1	11.4	83.5	13.0	92.7	15.5	88.5	14.8	82.0	13.5	78.6	12.9	76.7	12.7	73.8	12.1
AN + 20% Karinu	119.7	22.8	113.8	20.6	98.3	16.5	100.0	16.9	119.3	21.7	109.6	19.7	107.4	19.3	106.5	19.2	102.8	18.6
AN + 20% Vasalemma	74.6	10.7	109.3	19.2	130.2	24.2	132.8	24.8	130.4	24.3	135.0	25.3	140.4	26.6	148.8	28.6	140.7	26.8
AN + 20% Kurevere	106.3	18.1	108.5	18.9	125.5	23.0	123.8	22.6	116.6	21.1	108.3	19.2	97.9	16.9	30.2	1.7	57.9	8.2
AN + 20% Anelema	172.4	34.6	154.4	30.6	141.3	27.6	131.9	25.4	126.6	24.3	124.4	23.8	125.4	24.1	126.0	24.3	125.3	24.1
AN + 20% Anelema wastes	86.2	13.8	85.7	14.1	90.8	15.5	95.7	16.8	98.8	17.6	100.5	18.1	102.4	18.6	105.6	19.4	105.2	19.3
Step II																		
AN + 20% Võhmuta	292.9	40.8	178.8	21.4	156.3	17.4	174.2	19.3	171.9	19.5	201.9	23.9	264.0	33.2	212.7	26.1	210.5	26.0
AN + 20% Karinu	195.6	24.3	178.8	21.0	144.1	14.7	164.3	17.8	181.1	20.3	202.4	23.6	207.0	24.6	179.4	20.9	174.2	20.4
AN + 20% Vasalemma	180.1	21.8	182.9	21.8	175.8	20.2	170.2	19.2	172.2	19.6	167.2	19.0	169.2	19.5	185.5	22.2	189.6	23.0
AN + 20% Kurevere	106.2	12.4	67.7	4.9	59.7	3.1	70.9	5.2	86.5	7.9	105.2	10.9	104.5	10.9	85.2	8.0	63.9	4.9
AN + 20% Anelema	66.2	4.7	73.8	6.0	87.8	8.4	114.0	12.8	159.3	20.4	174.4	22.9	152.9	19.6	143.9	18.3	143.0	18.2
AN + 20% Anelema wastes	100.0	10.9	109.8	12.1	108.9	11.9	112.2	12.3	121.1	13.8	130.2	15.4	126.8	15.0	127.9	15.3	141.2	17.5

from 58.5 to 92.7 kJ mole^{-1} (pre-exponential factor A in between 1.3*10^3 and 5.4*10^6 s^{-1}), with Kurevere dolomite from 30.2 to 125.5 kJ mole^{-1} (A in between 5.5 and 9.7*10^9 s^{-1}). For step II (decomposition of Mg and Ca nitrates), the value of activation energy also varied in a great extent: for the AN blend with Võhmuta limestone from 156.3 to 292.9 kJ mole^{-1} (A in between 3.6*10^7 and 5.2*10^{17} s^{-1}) and with Anelema dolomite from 66.2 to 174.4 kJ mole^{-1} (A in between 1.1*10^2 and 8.8*10^9 s^{-1}) (Table 2). These results indicate that neither the decomposition of AN nor the interactions in the AN blends with limestone or dolomite additives follow a simple, but a complex reaction mechanism including stages with both lower and higher activation energies as compared to decomposition of neat AN.

Conclusions

No systematic dependence of the temperatures of endoeffect minimums on DTA curves corresponding to the principal transitions of $AN_{IV} \leftrightarrow AN_{III} \leftrightarrow AN_{II} \leftrightarrow AN_{I}$ on the heating rate were fixed, but the transition of $AN_{I} \leftrightarrow AN_{melt}$ was always shifted towards higher temperatures at higher heating rates.

These phase transitions at thermal treatment of neat AN were followed by the decomposition exotherm of AN in the temperature interval from 200 to 310 °C, thereby, the higher the heating rate, the more intensive the exotherm was.

At thermal treatment of AN blends with limestone or dolomite a multi-peaked endotherm was fixed on the DTA curves in the range of 180–280 °C, characterizing the interaction of AN with $CaCO_3$ and $MgCO_3$*$CaCO_3$ contained in natural limestone and dolomite. This endoeffect was followed, as a rule, by a more or less intensive exoeffect characterizing the decomposition of residual AN. The decomposition exotherm of AN was shifted towards higher temperatures and the intensities of these exotherms were much smaller as compared to neat AN, missing for some blends at the heating rate of 2 °C min^{-1} at all.

The endotherms in between 350 and 600 °C characterized the decomposition of previously formed $Mg(NO_3)_2$ and $Ca(NO_3)_2$.

The variation of the value of activation energy E along the reaction progress α shows the complex character of decomposition of AN, the interaction of AN with limestone and dolomite additives with formation of nitrates as well as the decomposition of the nitrates formed at previous stages.

For neat AN, the activation energy in the range of conversion (decomposition) degree of $0.1 < \alpha < 0.9$ ranges from 92.4 to 106.8 kJ mole^{-1}. For the blends of AN with limestone and dolomite, the value of activation energy in the same range of α varied in a greater extent than for neat AN—depending on the limestone or dolomite added for step I (decomposition and interactions of AN with limestone and dolomite additives) from 30.2 to 172.4 kJ mole^{-1}, for step II (decomposition of Mg and Ca nitrates) from 59.7 to 292.9 kJ mole^{-1}.

Acknowledgements This work was partly supported by Estonian Science Foundation (G7548).

References

1. Vyazovkin S, Clawson JS, Wight CA. Thermal dissociation kinetics of solid and liquid ammonium nitrate. Chem Mater. 2001; 13:960–6.
2. Oxley JC, Kauchik SM, Gilson NS. Thermal decomposition of ammonium nitrate-based composites. Thermochim Acta. 1989;153: 269–86.
3. Olszak-Humienik M. On the thermal stability of some ammonium salts. Thermochim Acta. 2001;378:107–12.
4. Oxley JC, Smith JL, Rogers E, Yu Ming. Ammonium nitrate: thermal stability and explosivity modifiers. Thermochim Acta. 2002;384:23–45.
5. Zeman S, Kohlíček P, Maranda A. A study of chemical micromechanism governing detonation initiation of condensed explosive mixtures by means of differential thermal analysis. Thermochim Acta. 2003;398:185–94.
6. Brower KR, Oxley JC, Tewari M. Evidence for homolytic decomposition of ammonium nitrate at high temperature. J Phys Chem. 1989;93:1029–33.
7. Koga N, Tanaka H. Effect of sample mass on the kinetics of thermal decomposition of a solid. Part 1. Isothermal mass-loss process of molten NH_4NO_3. Thermochim Acta. 1992;209: 127–34.
8. Koga N, Tanaka H. Effect of sample mass on the kinetics of thermal decomposition of a solid. Part 3. Non-isothermal mass-loss process of molten NH_4NO_3. Thermochim Acta. 1994;240:141–51.
9. Carvalheira P, Gadiot GMHJL, de Klerk WPC. Thermal decomposition of phase-stabilised ammonium nitrate (PSAN), hydroxyl-terminated polybutadiene (HTPB) based propellants. The effect of iron(III)oxide burning-rate catalyst. Thermochim Acta. 1995;269/270:273–93.
10. Simões PN, Pedroso LM, Portugal AA, Campos JL. Study of the decomposition of phase stabilized ammonium nitrate (PSAN) by simultaneous thermal analysis: determination of kinetic parameters. Thermochim Acta. 1998;319:55–65.
11. Kaljuvee T, Edro E, Kuusik R. Influence of lime-containing additives on the thermal behaviour of ammonium nitrate. J Therm Anal Cal. 2008;92:215–21.
12. Friedman HL. Kinetics of thermal degradation of char-forming plastics from thermogravimetry. Application to a phenolic plastic. J Polym Sci. 1965;6C:183–95.
13. Flynn IH, Wall LA. A quick, direct method for the determination of activation energy from thermogravimetric data. Polym Lett. 1966;4:323–8.
14. Ozawa T. Kinetic analysis of derivative curves in thermal analysis. Therm J. Anal Cal. 1970;2:301–24.
15. Vyazovkin S. Model-free kinetics. Staying free of multiplying entities without necessity. J Therm Anal Cal. 2006;83:45–51.
16. AKTS AG. AKTS Software and SETARAM Instruments: a global solution for kinetic analysis and determination of the thermal stability of materials. Siders: AKTS AG; 2006. 88 pp.